Int. J. Electrochem. Sci., 17 **(2022)** Article Number: 221211, doi: 10.20964/2022.12.14

International Journal of
ELECTROCHEMICAL
SCIENCE
www.electrochemsci.org

Electrochemical Treatment of Industrial Effluent and Its Impact on Stainless Steel Corrosion

Ehab S. Gad[1,*], *Mohamed A. Abbas*[2], *Maha Abdelkreem*[3], *Ayman H. Ahmed*[1]

[1] Chemistry Department, College of Science and Arts, Jouf University, Gurayat, Saudi Arabia
[2] Egyptian Petroleum Research Institute, 11727 Cairo, Egypt
[3] Chemical Engineering Dept. High Technological institute, 10th of Ramadan city, Egypt
[*]E-mail: esgad@ju.edu.sa

Received: 4 September 2022 / *Accepted:* 24 October 2022 / *Published:* 17 November 2022

Controlling environmental problems and treating wastewater are major concerns. In the last decade, electrochemical coagulation has arose as the most effective wastewater treatment process when compared to traditional wastewater treatment techniques. A laboratory scale electrocoagulation (EC) process was used in this study to treat industrial dye effluent via ongoing anodic dissolution of stainless steel anode for artificially aerated galvanic cells. To achieve the highest possible treatment efficiency, two essential parameters such as treatment time (15, 30, 45, and 60 min) and applied potential (400, 750, 900, 1200 mV) was assessed. To verify the effectiveness of the purification method, physicochemical analysis, ultraviolet (UV) spectroscopy, and Fourier transform infrared (FTIR) analysis were used. High decolourization efficiency was achieved under ideal conditions, reaching more than 91 percent color removal. The obtained results from all the previous techniques revealed that the optimal dye removal conditions are as follows: 60 minutes and 1200 mv applied potential. To detect the corrosion influence of the treated dye effluent (at different conditions) on the stainless steel, some of the electrochemical measurements (Potentiodynamic polarization PDP, and electrochemical impedance EIS) and morphological investigation (scanning electron microscope (SEM) and energy dispersive X-ray (EDX)) were also applied. It is showed that the more purity of the dye effluent, the less corrosion rate obtained. Finally the electrocoagulation process achieved good results in the purification of dye wastewater.

Keywords: Electrocoagulation, decolourization, dye effluent, impedance, polarization.

1. INTRODUCTION

Dyes are a major source of concern due to its extensive use, hazardous aromatic residues (such as aromatic amines), and bio-resistance to conventional anoxic wastewater management [1–3]. One of the most challenging industrial wastewaters to handle is dye effluent from the textile industry. Various dyes used throughout the textile industry typically have complex aromatic structures and chemically

synthesized origins, which make them more stable and harder to breakdown. The three primary categories of synthetic dyes are anionic, cationic, and nonionic (disperse dyes). The common function group that present in anionic and nonionic dyes and cause the color are often azo or anthraquinone [3]. Xanthene dyes are mostly used extensively in the textile industry, biological stains, and cosmetic products [4]. Because of their fused aromatic structures, anthraquinone-based dyes are more difficult to degrade. Because the remaining dye in dye wastewater does not adhere to the fabric, it produces highly colored effluent. Because of the non-attachment to the textiles, 10-15percent of the dye used in the process remains in the effluent. However, the fact that the majority of dyestuffs are poisonous, cytotoxic, and genotoxic is frequently disregarded. [5, 6]. They also are environmentally destructive due to their strong bonds that have the possibility for persistence and deposition in the environment [5]. The recycling of industrial wastewater has received a lot of attention among other water management options [7, 8]. The treated wastewater has a numerous advantages over conventional water sources, including a reduction in pollution, the ability to artificially replenish groundwater reserves, and the provision of an adequate nutrient demand for irrigation in landscaping and agriculture [7]. A number of methods, including reverse osmosis and the adsorption approach [9, 10], are therefore beneficial in the treatment of effluents to remove dyes. However, those previous were constrained by the significant amounts in reject streams combined with the low concentration ranges that can be handled. Extra thought is also prompted by the high expense of photooxidation and ozonation. EC is a simple and low-cost method for treating dye effluents [1]. EC uses various substances as sacrificial anodes, such as Al and Fe, to generate positively charged ions that can form metal hydroxide agglomerates. Charge neutralization allows iron ions to completely separate dye from aqueous solutions. Metallic hydroxide agglomerates can also be used to remove dyes via bonding or sweep coagulation [11, 12]. The majority of electrocoagulation research has focused not only on Fe and Al anodes, but also stainless steel anodes is used to remove textile wastewaters [13, 14], and other organic particles [15, 16]. Significant variables influencing dye removal by EC include the kind of dye, electrode area and material, used current, solution acidity, and stirring speed [12, 17]. Solution pH, for example, influences the creation of (OH^-) and also the transformation of Fe (II) to Fe (III) ions throughout EC [18]. The electrode material controls the reactions that take place during the EC process [19]. The electrode materials chosen are determined by the species to be eliminated as well as the properties of the electrolyte. Stainless steel, for instance, is discovered to be a good electrode for color removal. Ming-Chi Wei et al [20] reported the removal of azo, anthraquinone, and xanthene dyes (as Acid Black 1, Reactive Blue 4, and Eosin Yellow respectively) using EC with various types of low-cost steel wool cathode. Also, at all pH values and current densities studied, in just the first five minutes of EC, reactive dye bath effluents completely decolored utilizing stainless steel [21]. Similar results were obtained when dyes were treated [22, 23]. The purpose of this study is to evaluate the dye effluent quality before and after treating it with the electrocoagulation (EC) technique. FTIR, UV adsorption, scanning electron microscopy, and EDX techniques were used to assess the level of water treatment. The influence of *E* and immersion time on the corrosion performance of stainless steel under the conditions of wastewater containing textile dyeing discharge were investigated using various electrochemical techniques.

2. MATERIALS AND METHODS

2.1. Samples collection:

A sample of industrial effluent was taken from one of the most well-known dyeing companies. The samples were taken from the end of the manufacturing line, which contained all possible sorts of pollutants emitted by these industries. Before using any treatment technology, the samples were thoroughly evaluated (physically and chemically).

2.2. Electrocoagulation treatment method

Many EC batch trial runs were done in the laboratory after extensive evaluation of raw wastewater. To homogenize the sample, the effluent was first vigorously agitated for several minutes with a stirrer. A glass container with a capacity of 500 ml is included in the simulation model of the experimental setup in fig 1. It consists of an anode, a cathode and power supply. Both the anode and the cathode were made of the stainless steel grade 304, which contains: 18% to 20% Cr, 8% to 10.5% Ni, 0.08% C, 2% Mn, 0.75% Si, 0.045% P, 0.03% S, and 0.1% N. EC processing was performed using different times (15-60 min) and different voltage (400-1200 mV).

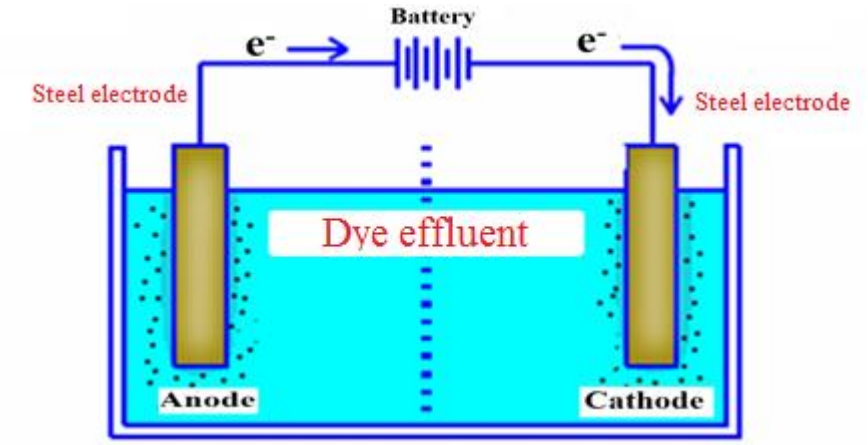

Figure 1. Scheme of the experimental setup of electrocoagulation cell.

2.3. Evaluation Methods

2.3.1. Physicochemical analysis of wastewater

The pH levels were determined using a Hanna instrument. The measurement was performed using a spectrophotometer (Model HACH DR 6000). Biological oxygen demand (BOD) values were calculated using the Lovibond incubator in accordance with standard techniques [24]. The standard procedure was used to determine TSS from an unfiltered sample.

2.3.2. Ultraviolet spectrum measurements

The visible spectrum was used to evaluate the untreated wastewater and electrochemically treated samples. The dye concentration in textile effluent was determined using a UV-Visible spectrophotometer (Model Jasco V-630) at the maximum absorbance band of 650 nm. The formula, as stated in Eq. (1), was used to calculate dye effluent decolorization after electrocoagulation processing.

$$\text{Dye effluent decolourization (\%)} = [(A_i - A_f)/A_i]*100 \quad (1)$$

where A_i and A_f represented the dye absorbance prior to and after EC respectively.

2.3.3. FTIR analysis

Using a FTIR spectrometer (Bruker, Alpha-E) in the 500–4000 cm^{-1} range, the functional groups contained in the dye effluent before and after EC was identified.

2.3.4. Surface analysis

SEM and EDX Spectroscopy (zeiss gemini sigma 300 vp, Japan) is used to carry out surface morphology research and the elemental analyses respectively. SEM and EDX analysis has been performed on the stainless steel samples before (blank) and after electrocoagulation process (anode and cathode) at 1200 mV and after 60 min of immersion time.

2.4. Electrochemical evaluation

Electrochemical techniques (PDP and EIS) were used to evaluate the treated water as corrosive media on the stainless steel as working electrode through the electrochemical cell fig. 1. By coupling the electrochemical cell with three electrodes (working electrode, reference electrode, and counter electrode) to a Volta lab master egz301 that was controlled by a computer for continuous monitoring and analysis, measurements for EIS and PDP curves were taken. At 25 ^{o}C, all the electrochemical evaluations were done. Ten points were taken into account for EIS measurements for every decade of frequency that fell between 100 kHz and 100 mHz. At a scan rate of 2mV/min and between -800 mV and -300 mV, PDP curve measurements were performed.

3. RESULTS

3.1. Physicochemical properties of wastewater

Table 1 lists the characteristics of the raw wastewater utilized in the studies. When compared to the properties of ordinary domestic wastewater, the average BOD, COD, and TSS levels are on the moderate strong side.

Table 1. Physico-chemical properties of treated and untreated industrial effluent samples.

Experiments analysis	Dye effluent sample	400 mV	750 mV	900 mV	1200 mV
Temperature	25	25	25	25	25
T.S.S. (mg/l)	800	470	111	76	18
pH	5.0	6.1	6.5	6.7	7.1
T.D.S (mg/l)	7650	4700	2390	980	490
B.O.Ds (mg/l)	4730	3500	2420	540	100
C.O.D (mg/l)	9850	6345	3194	1200	240
Conductivity (µ.s)	14850	12500	5480	970	800
Nitrate (mg/l)	102.4	71.3	52.4	22.4	18.1
Phosphate (mg/l)	25.61	15.7	2.64	1.3	0.34
Sulfide (mg/l)	10	5.78	1.48	0.87	0.36
Oil & Grease (mg/l)	43	18	20	11	3
Color	Dark Pink	Light Pink	Light Pink	Nearly Colorless	Nearly Colorless

The large values of TDS, and conductivity of wastewater, are beneficial to EC treatment because it eliminates the requirement to use an electrolyte to enable current flow in the effluent solution. In the case of electrocoagulation (EC), the anodic dissolution of the stainless steel electrode within the electrolytic cell promotes the generation of ferrous ions (Fe(II)/Fe(III)), which interact with hydroxide ions in solution to form $Fe(OH)_2(s)$ and $Fe(OH)_3(s)$. Again for suspended particles to construct flocs, these hydroxides behave as a coagulant. The enormous surface area of these agglomerates is beneficial for the quick adsorption of organic color components found in dye effluent as well as the capture of suspended particles that silt or float subsequently [25]. Table 1 gives the physicochemical characteristics of textile effluent prior to and after EC at various potentials (400, 750, 900, and 1200 mV) and exposure times (60 min). To assess the efficiency of the EC process, many values were measured and recorded in table 1. Total Suspended solids (TSS), pH, total dissolved solids (TDS), conductivity, chemical oxygen demand (COD), (BOD), the concentrations of some anions (S^{2-}, PO_4^{3-}, and NO_3^-) and finally the content of oil and grease were assessed both before and after treatment. The studied parameters provided an early indication of the purification process's success. Total suspended solids (TSS) dropped gradually from 800 mg/L in the untreated sample to 18 mg/L after 60 minutes of coagulation with increasing applied potential till 1200 mV. Electrocoagulation can lower TSS levels by interacting with negatively charged oxy/hydroxy-metal ions created in the process to destabilize colloidal particles with positive surface charges [26]. Also total dissolved solids (TDS) lowered from 10700 mg/L in the wastewater sample to 490 mg/L at 1200 mV applied potential and after 60 min of the coagulation process. The findings also obviously demonstrate that the presence of soluble substances in the effluent is indicated by the high electrical conductivity (14850 µ.s) of the wastewater recorded (800 µ.s) with the influence of the EC process under the conditions specified (60

min and 1200 mV). The amount of oxygen usually needed by microorganisms to decompose organic substance known as biochemical oxygen demand (BOD), which can be calculated for diluted and undiluted specimens. The BOD values are determined by the amount of dissolved organic matter in the examined water samples. The more organic matter there is, the more oxygen microbes need to breakdown it. Chemical oxygen demand (COD) is the total quantification of all chemicals (organics and inorganics) in samples collected and can be evaluated using a strong oxidizing chemicals (such as $K_2Cr_2O_7$) to degrade both organic and inorganic particles introduce in wastewater samples. Furthermore, COD values always seem to be larger than BOD values because COD involves both biodegradable and non-biodegradable compounds, whereas BOD only includes biodegradable substances. The final COD value drops from 9850 to 240 mg/L, while the BOD value drops from 4730 to 100 mg/L of O_2. The analysis also revealed a gradual decrease in the concentration of certain categories of anions found in dye effluent. Nitrate levels have been reduced from 100 to 18.1 mg/L, phosphate levels from 25 to 0.35 mg/L, and sulfide levels from 10 to 0.36 mg/L. Finally, table 1 clearly demonstrates that the colored effluent is nearly pollution-free. All previous values appeared to be primarily concerned with the success of the EC process. The dissolution of the anode, which releases an electron from its surface and causes metals to change into metal hydroxide, is the primary cause of the coagulation process. Metal hydroxide then precipitates or is adsorbed on the surface of the cathode.

3.2. UV-VIS Spectrophotometry Analysis

Table 2 represents the percentage of dye wastewater decolorization after electrocoagulation (EC) processing at various electrical potential ranges (400, 750, 900, and 1200 mV at constant time) and exposure durations (15, 30, 45, and 60 min at constant potential) using UV-VIS spectra.

Table 2. UV spectrophotometer of treated samples at different times (15-60 min) and different. Voltage (400-1200 mV).

Time (min)	**Voltage (mV)**			
	400	**750**	**900**	**1200**
	(%) dye effluent decolourization			
15	**15.41**	**17.39**	26.14	58.06
30	19.08	26.25	27.07	83.80
45	20.00	28.06	29.29	90.26
60	35.03	40.25	72.82	**91.25**

A direct relationship has been shown in table 2, which is depicted in fig. 2. The percentage of dye effluent decolorization increases with increasing electrocoagulation duration for the same voltage, as well as with rising electrical potential values between the anode and cathode at constant time. At

1200 mV for 60 minutes, the highest percentage of dye elimination (91.25%) was attained (the optimum condition for EC).

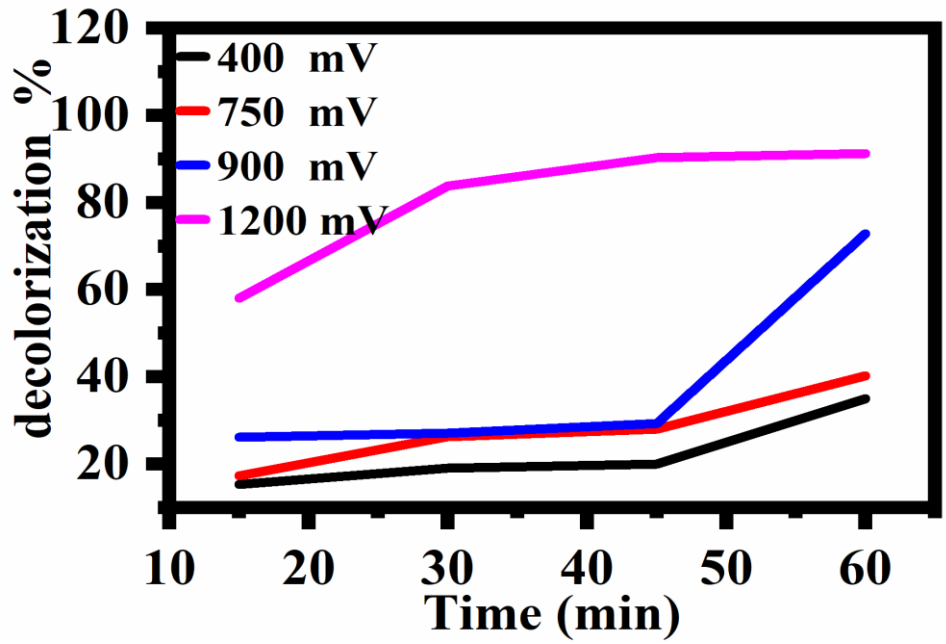

Figure 2. Decolorization % of treated samples at different voltage (400-1200 mV) for different time (15-60 min)**.**

3.3. Characterization using FTIR

The IR spectra reveal that during the electrocoagulation process, some structural reforms may also have taken. The FT-IR spectra of the studied industrial dye effluent before (fig. 3a) and after electrolysis (fig. 3b) show multiple distinct bands in the spectra. To estimate the impact of applied potential on dye removal effectiveness, the FTIR spectrum of the treated samples was examined at various voltage values (400, 750, 900, and 1200 mV) during the same working time (60 minutes). The dye removal efficacy is demonstrated by a qualitative and quantitative comparison of the produced peaks for both treated and untreated samples. The apparent bands at 1057 cm^{-1} display C-O stretching, denoting primary alcohol [27], and then the peak at 1540 cm^{-1}, which is typical of N-O stretching, indicating nitro compounds, 1699 cm^{-1} peak could be due to C=O stretching for conjugated aldehyde, and finally bands at 2921 cm^{-1} peak due to C-H stretching for alkane. All the above mentioned peaks (C-O, N-O, C=O, and C-H) are characteristics for the dye molecules dissolved in the untreated samples. Water molecules are indicated by a peak at 3450 cm^{-1} (3000-3500 cm^{-1}) in the after-treatment process, O-H stretching and bending, respectively [28]. H-O-H stretching vibrations may be seen in the sharp peaks at 1637.49 cm^{-1} and 1636.38 cm^{-1}. The stretching of aliphatic ether causes the peak at 1120 cm^{-1}. The absence of peaks at 1057 cm^{-1}, 1540 cm^{-1}, 1699 cm^{-1}, and 2921 cm^{-1} in the spectrum of treated samples indicated that numerous chemical species had already been eliminated. The proportional intensities of the specimens of different voltages are clearly shown in fig. 3b. The intensity of the peaks declined with increasing potential until 1200 mV, as seen in the figure.

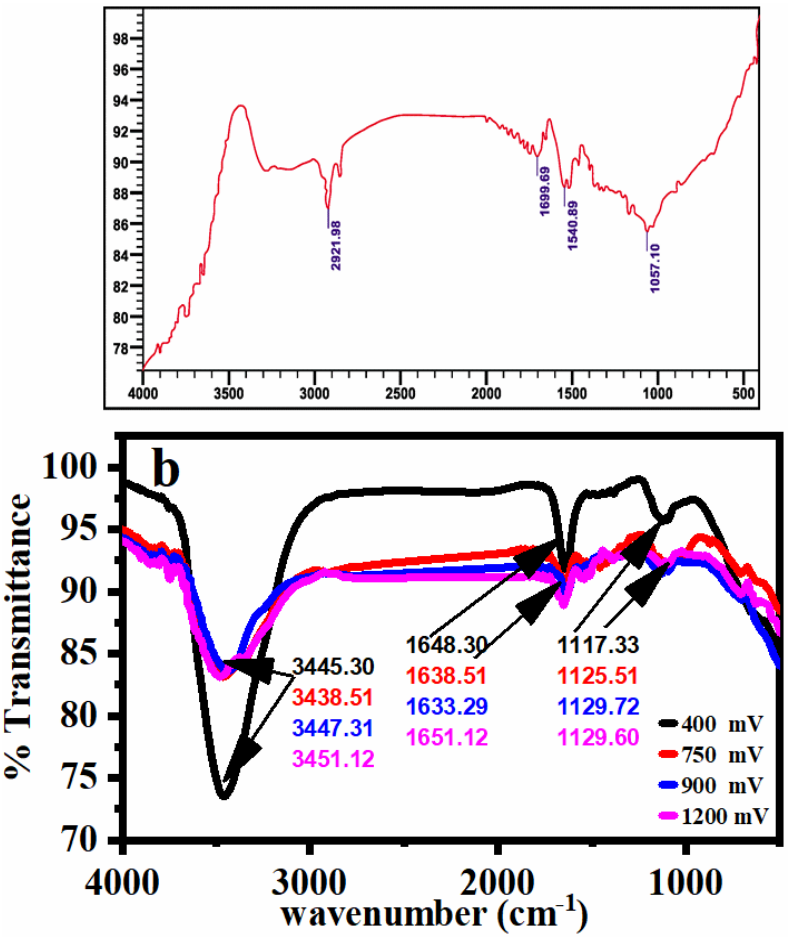

Figure 3. FTIR spectrum for (a) untreated (b) treated samples at different voltage (400-1200 mV).

3.4. SEM and EDX

SEM and EDX were used to examine the surface morphology and elemental analysis of stainless steel electrodes both before and after the treatment process. Surface morphology of stainless steel before electrocoagulation (blank), after exposure time as anode, and cathode in electrocoagulation cell with similar magnification power are shown in figures 4a, 4b and 4c.

Before the dye treatment, the stainless steel surface was smoother (fig. 4a). Moreover as shown in the micrograph (fig. 4b), the anode surface is corroded due to oxidation of stainless steel into Fe ions because of the acidic pH as well as the aggressive constituent present in the untreated wastewater sample (table 1). In contrast, in fig 4c, the accumulation of dye molecules at the cathode with very small particle sizes is clearly seen (Nano scale). The EDX peaks showed the presence of the distinct elements of the blank, anode and cathode in figs 4a, b and c, respectively. Iron and other stainless steel components (Mn, Ni, Cr, and C) were found in the anode peaks, as well as the O peak, which was the major component of the corrosion product. In fig. 4c, the peaks of the elements that make up the organic dye (C, N, O, and S) are clearly visible, as evidenced by the FTIR spectrum. Finally, by comparing the intensity of the iron peak in the three samples, we can see that the intensity of the Fe peak dropped in the cathode sample due to dye molecules accumulating on the stainless steel surface.

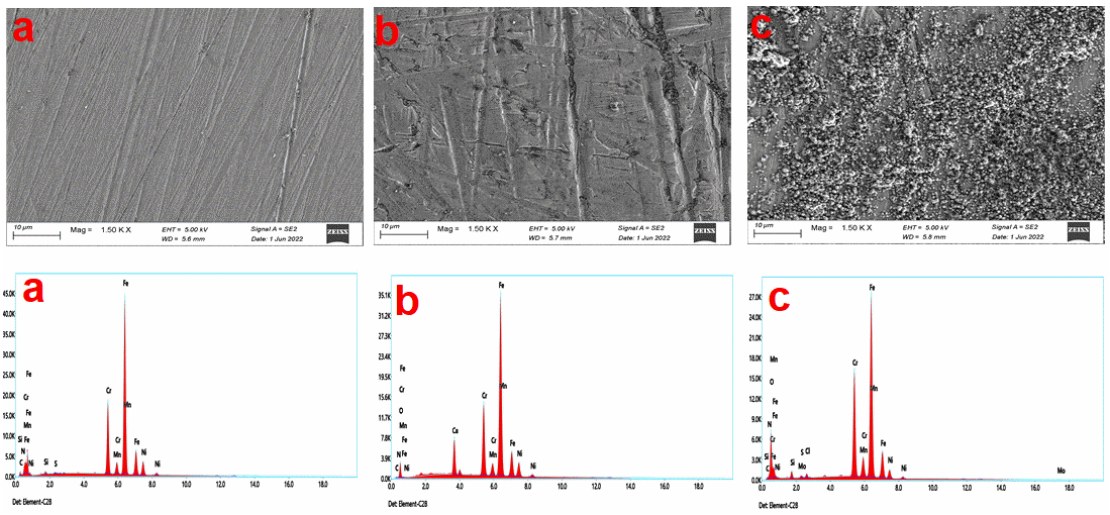

Figure 4. SEM and EDX micrographs for stainless steel surface without treatment (a) blank (b) anode, and (c) cathode at 1200 mV.

3.5. Impact of dye effluent on stainless steel corrosion

3.5.1. Potentiodynamic polarization (PDP) investigations

Using PDP curves, the corrosion mechanisms in wastewater, involving textile dyeing effluent before and after electrocoagulation techniques, as well as their effect on stainless steel, were examined.

Table 3. PDP parameters for dye effluents at different times of (15-60 min) and different voltage (400-1200 mV) of electrocoagulation process.

	Potential (mV)	Time (min)	E_{corr} (mV)	i_{corr} (µA/cm²)	R_p (kohm.cm²)	β_a mV/ decade	β_c mV/ decade	C_R µm/Y
Before			-673	26.8	3.39	281	-290	313
After	400	15	-619	10.5	3.02	124	-293	123
		30	-617	10.4	3.63	157	-340	121
		45	-612	9.4	4.47	186	-327	110
		60	-581	8.96	3.35	121	-269	105
	750	15	-600	8.4	4	130	-340	98
		30	-590	7.9	4.37	134	-534	92
		45	-578	7.6	4.87	132	-443	89
		60	-575	7.5	3.82	107	-337	88
	900	15	-593	7.2	5.24	157	-324	84
		30	-571	6.9	7.75	147	-339	81
		45	-567	6.8	6.39	131	-331	79
		60	-559	6.34	6.29	136	-380	74
	1200	15	-583	5.95	5.87	119	-312	70
		30	-559	5.7	6.98	127	-364	67
		45	-520	5.6	5.62	119	-308	66
		60	-499	4.4	9.13	122	-354	52

After the electrocoagulation operations, using different applied potentials (400, 750, 900, and 1200 mV) for varied times (15, 30, 45, 60 min), polarization parameters were measured. Fig. 5 depicts representative stainless steel PDP curves in multicomponent wastewater before and after coagulation procedures. The corrosion current density, i_{corr}, and corrosion potential, E_{corr}, were estimated using PDP data and are displayed in table 3.

As shown in fig. 5 and table 3, the largest corrosion current and hence corrosion rate of stainless steel in dye wastewater was recorded before electrocoagulation processes, as evidenced by the recorded values of the corrosion parameters [29]. Longer treatment immersion times resulted in lower corrosion rates for the same potential, which might be explained by an increase in the elimination rate of corrosive components present in wastewater as time passes at the same potential [30]. For example, at 400 mV applied potential, the corrosion current firstly decreased from 26.8 µA/cm² to 10.5 µA/cm² after 15 min reaching 8.9 µA/cm² at 60 min. The solution pH rises throughout EC as a response of hydrogen evolution at the cathode [31]. So, the acidity of the treated wastewater decrease with the time as seen in table 1, hence the corrosion rate decreased with the time. On the other side, it is appeared from the results in table 3, the inverse relation between the applied potential in treatment process versus corrosion rate (C_R). The corrosive behavior of the treated dye effluent was the lowest at 1200 mV and 60 min (EC conditions) reaching corrosion rate equal to 52 µm/Y. A current density (i_{corr}) is shown to be lesser in extensively treated samples, and this continues to high potentials (E_{corr}), these results indicate providing a longer wastewater treatment.

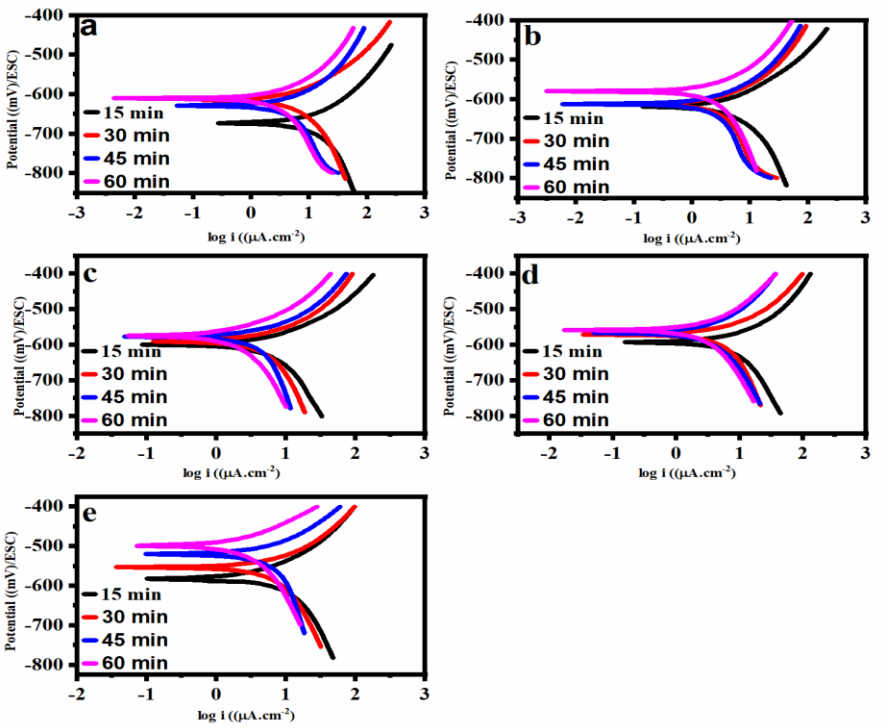

Figure 5. PDP curves for dye solution (a) before treatment, and after treatment at different applied potential (b) 400 mV (c) 750 mV, (d) 900 mV, and (e) 1200 mV.

EIS is an efficient technique for assessing the formation of corrosion products and electrochemical processes at the anodes/electrolyte interface. The oxide film production on the stainless steel surface in aerated industrial wastewater, including textile dyeing effluent before and after coagulation procedures, is monitored by recording EIS spectra at the open circuit potential after different immersion times (15, 30, 45, 60 min) using different applied potentials (400, 750, 900, and 1200 mV). Fig. 6 shows the results of impedance measurements taken with the stainless steel electrode in the form of Nyquist plots. The impedance response has a single semicircle, which corresponds to one time constant, as shown in the graphs. The stainless steel Nyquist plot shows small semicircles at high and intermediate frequencies, as seen in fig. 6. The high-frequency area is assumed to be linked to charge transfer and double layer capacitance. The treated wastewater does not modify the impedance form, but it increases the diameter of this semicircle when compared to untreated wastewater.

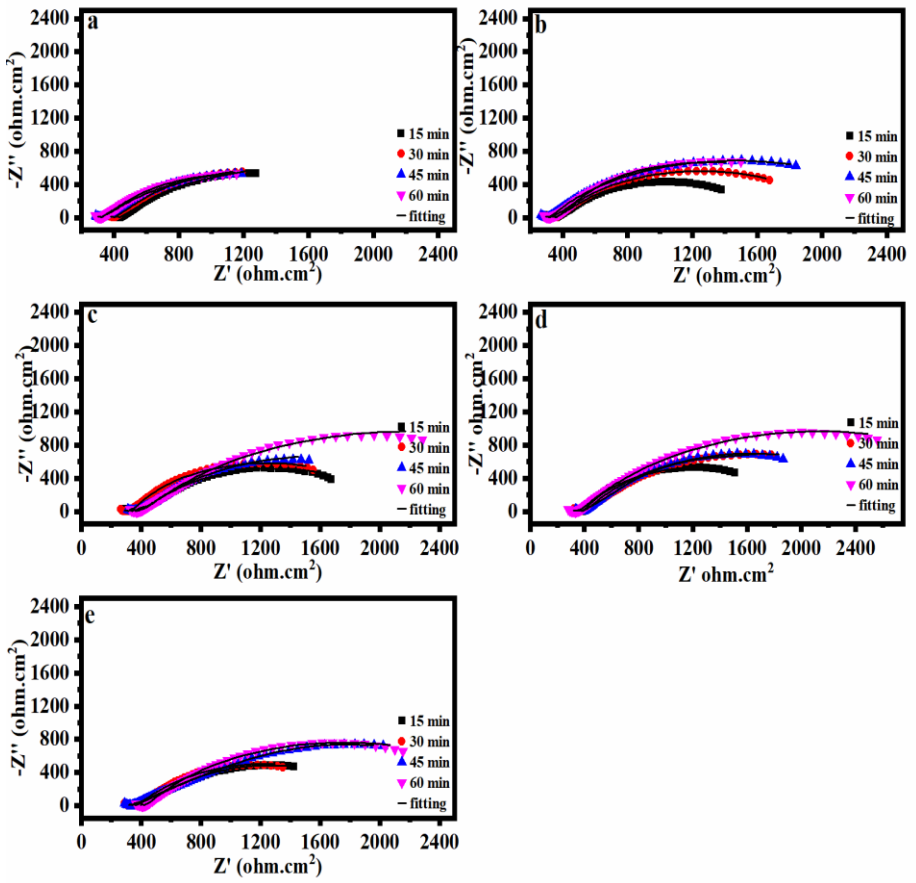

Figure 6. Nyquist impedance plots for dye solution (a) before treatment, and after treatment at different applied potential (b) 400 mV (c) 750 mV, (d) 900 mV, and (e) 1200 mV.

The diameter grows in lockstep with increasing the treatment time (up to 60 min) and voltage (up to 1200 mV). Then, suggesting an increase in the products' corrosion and inhibition resistance. A faradic process using a single charge transfer resistance in parallel with the double-layer capacitance element was ascribed to the presence of a single capacitive loop [32]. This indicated that charge

transfer occurs at the stainless steel/solution contact, and the manner of charge transfer controls corrosion reaction [33]. The semicircles' non-homogeneous nature is a feature of solid electrodes; such frequency dispersion has been attributed to stainless steel electrode micro-roughness and other inhomogeneity [34]. The related circuit was acquired utilizing the EIS analyzer once more for the obtained analysis of EIS, as shown in fig. 7. The phase constant element (Q_{cdl}) is only equivalent to the double layer capacitance, the solution resistance is (R_s), and the charge transfer resistance is (R_{ct}). Table 4 shows the findings of fitted spectra, which reveal that the R_s values are quite tiny in relation to the R_{ct} values. EC process enhances R_p and R_{ct} and lowers C_{dl} (the magnitude of the double layer capacitance) for dye effluent.

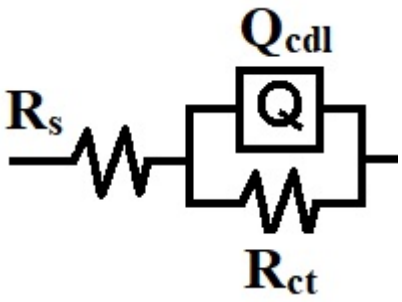

Figure 7. Equivalent circuits compatible with the experimental impedance data in Figure 6 for (a) before treatment, and after treatment at different applied potential (b) 400 mV, (c) 750 mV, (d) 900 mV, and (f) 1200 mV.

Table 4. The impedance parameters for dye effluents at different times of (15-60 min) and different voltage (400-1200 mv) of electrocoagulation process.

	Potential (mV)	**Time (min)**	**R_s ohm.cm²**	**Q x10^{-4} (S Sec^{n}m^{-2})**	**n**	**C_{dl} µF/cm²**	**R_{ct} ohm.cm²**
Before			435	9.21	0.65	1400	2349
After	400	15	362	6.87	0.69	860	2399
		30	360	5.19	0.75	579	2680
		45	314	3.8	0.76	384	2709
		60	330	3.72	0.80	374	2747
	750	15	349	5.16	0.75	567	2509
		30	316	4.78	0.76	527	2850
		45	390	3.42	0.78	352	3221
		60	369	3.30	0.83	345	3790
	900	15	382	5.04	0.76	552	2654
		30	391	4.31	0.79	461	2980
		45	387	2.92	0.80	293	3456
		60	345	2.71	0.84	273	3860
	1200	15	422	4.72	0.78	512	2832
		30	344	3.55	0.80	364	3125
		45	351	2.63	0.82	261	3654
		60	368	2.34	0.85	233	4132

This impact appears to be proportional to the exposure time and applied potential, indicating that the establishment of a protective layer on the stainless steel surface and the creation of a mass and charge transfer barrier successfully prevent corrosion [35]. As resulted from different evaluation techniques in this research, the best color degradation conditions of concentrated dye effluent were at 60 min and 1200 mV.

4. CONCLUSIONS

The findings show that the EC procedure with stainless steel electrodes (anode and cathode) is a very effective and cost-effective treatment for industerial wastewater. The electrocoagulation method at various periods and voltages resulted in good color degradation of concentrated dye effluent. It can be inferred that under the optimal conditions of a 60-minute coagulation period and a 1200 mV applied voltage, a maximum of 91.25 percent color removal was achieved. FT-IR analysis confirmed that a high level of dye degradation was attained during the investigation. The elimination of organic dyes from aqueous solution is confirmed by the UV-Vis spectrum. The morphological changes, as well as the oxidation of the anode and the chemical attraction of dye molecules at the cathode, are confirmed by SEM and EDX tests. The treated solutions had a minor corrosion effect on stainless steel, according to PDP and EIS tests.

ACKNOWLEDGMENTS
This work was funded by the Deanship of Scientific Research at Jouf University under grant No (DSR-2021-03-03166)

References

1. C. A. Martínez-Huitle, and E. Brillas, *Appl. Catal.* B, 87 (2009) 105.
2. M. Eyvaz, M. Kirlaroglu, T. S. Aktas, and E. Yuksel, *Chem. Eng. J.*, 153 (2009) 16.
3. E. Forgacs, T. Cserháti, and G. Oros, *Environ. Int.*, 30 (2004) 953.
4. H. Zheng, Y. Pan, and X. Xiang, *J. Hazard. Mater*., 141 (2007) 457.
5. K. S. Wang, H. Y. Chen, L. C. Huang, Y. C. Su, and S. H. Chang, *Chemosphere*, 72 (2008) 299.
6. S. H. Chang, S. H. Chuang, H. C. Li, H. H. Liang, and L. C. Huang, *J. Hazard. Mater*., 166 (2009) 1279.
7. M. Saleem, *Int. J. Environ. Eng*., 1 (2009) 306.
8. M. M. Ruma, and A.U. Sheikh, *African J. Environ. Sci. Technol*., 4 (2010) 028.
9. E. S. Gad, M. Owda, and R. Yahia, *Egypt. J. Chem*., 63 (2020) 2075.
10. A. M. Yousif, E. S. Gad, and H. El-Sharary, *Egypt. J. Chem*., 64 (2021) 7195.
11. M. M. Emamjomeh, and M. Sivakumar, *J. Environ*. *Manage*., 90 (2009) 1663.
12. B. Merzouk, B. Gourich, A. Sekki, K. Madani, Ch. Vial, and M. Barkaoui, *Chem. Eng. J*., 149 (2009) 207.
13. N. Ardhan, P. Tongpadungrod, and C. Phalakornkule, *Mater. Today: Proc.*, 52 (2022) 2529.
14. E. Yuksel, M. Eyvaz, and E. Gurbulak, *Environ. Prog. Sustain. Energy*, 32 (2013) 60.
15. T. Olmez–Hanci, Z. Kartal, and I. Arslan–Alaton, *J. Environ. Manag*., 99 (2012) 44.

16. N. Modirshahla, M. A. Behnajady, and S. Mohammadi–Aghdam, *J. Hazard. Mater*., 154 (2008) 778.
17. P. Durango-Usuga, F. Guzmán-Duque, R. Mosteo, M.V. Vazquez, G. Peñuela, and R.A. Torres-Palma, *J. Hazard. Mater*., 179 (2010) 120.
18. Y. Gendel, and O. Lahav, *J. Hazard. Mater*., 183 (2010) 596.
19. M. Y. A. Mollah, R. Schennach, J. R. Parga, and D. Cocke, *J. Hazard. Mater*., 84 (2001) 29.
20. W. Ming-Chi, W. Kai-Sung, H. Chin-Lin, C. Chih-Wei, C. Tsung-Jen, L. Shiuan-Shinn, and C. Shih-Hsien, *Chem. Eng. J.*, 192 (2012) 37.
21. I. Arslan-Alaton, I. Kabdasli, B. Vardar, and O. Tuenay, *J. Hazard. Mater*., 164 (2009) 1586.
22. I. Kabdasli, B. Vardar, I. Arslan-Alaton, and O. Tuenay, *Chem. Eng. J.*, 148 (2009) 89.
23. P. SenthilKumar, N. Umaiyambika, and R. Gayathri, *Environ. Eng. Manage. J.*, 9 (2010) 1031.
24. S. Jouanneau, L. Recoules, M. J. Durand, A. Boukabache, V. Picot, and Y. Primault, *Water Res.*, 49 (2014) 62.
25. M. Saleem, A. A. Bukhari, and M N. Akram, *J. Basic Appl. Sci*., 7 (2011) 11.
26. H. Afanga, H. Zazou, F. E. Titchou, Y. Rakhila, R. A. Akbour, A. Elmchaouri, J Ghanbaja and M. Hamdani, *Sustainable Environ. Res.*, 30 (2020) 11.
27. M. Hernandez-Ortega, T. Ponziak, C. Barrera-Diaz, M. A. Rodrigo, G. Roa-Morales, and B. Bilyeu, *Desalination*, 250 (2010) 144.
28. S. Raghu, C. Woo Lee, S. Chellammal, S. Palanichamy and A. Basha C., *J. Hazard. Mater*., 171(2009) 748.
29. A. Dura, and C. B. Breslin, *J. Hazard. Mater*., 374 (2019) 152.
30. M. A. Abbas, M. A. Bedair, O. E. El-Azabawy, and E. S. Gad, *ACS Omega*., 6 (2021) 15089.
31. N. Hashem, E. S. Gad, M. EL-Rabiei, and A. Bahrawy, *Egypt. J. Chem*., 64 (2021) 5037.
32. M. A. Bedair, S. A. Soliman, M. F. Bakr, E. S. Gad, H. Lgaz, C. Ill-Min., M. Salama, and F. Z. Alqahtany, *J. Mol. Liq*., 317 (2020) 114015.
33. X. Li, S. Deng, and H. Fu, *Corros. Sci*., 55 (2012) 280.
34. I. M. Nassar, M. A. Abbas, A. hamdy, and O. E. Elazabawy, *Int. J. Curr. Res*., 5 (2013) 4327.
35. K. F. Khaled, *Mater. Chem. Phys*., 112 (2008) 290.

© 2022 The Authors. Published by ESG (www.electrochemsci.org). This article is an open access article distributed under the terms and conditions of the Creative Commons Attribution license (http://creativecommons.org/licenses/by/4.0/).